Supporting Information

Au Nanobead Chains with Tunable Plasmon Resonance and Intense Optical Scattering: Scalable Green Synthesis, Monte-Carlo Assembly Kinetics, DDA Modeling and Nano-Biophotonic Application

Authors: Alan McLean[1], Michael Kanetidis[2], Tarun Gogineni[1], Rahil Ukani[1], Ryan McLean[1], Alexander Cooke[1], Inbal Avinor[1], Bing Liu[3], Panos Argyrakis[2x], Wei Qian[1,3x], Raoul Kopelman[1x]

1. University of Michigan, Department of Chemistry, 930 N University Ave, Ann Arbor, MI 48109, USA
2. Aristotle University of Thessaloniki, Department of Physics, A.U. Th. Campus, Thessaloniki, 54124, Greece
3. IMRA America, Inc., 1044 Woodridge Ave, Ann Arbor MI, 48105, USA

[x]Corresponding authors

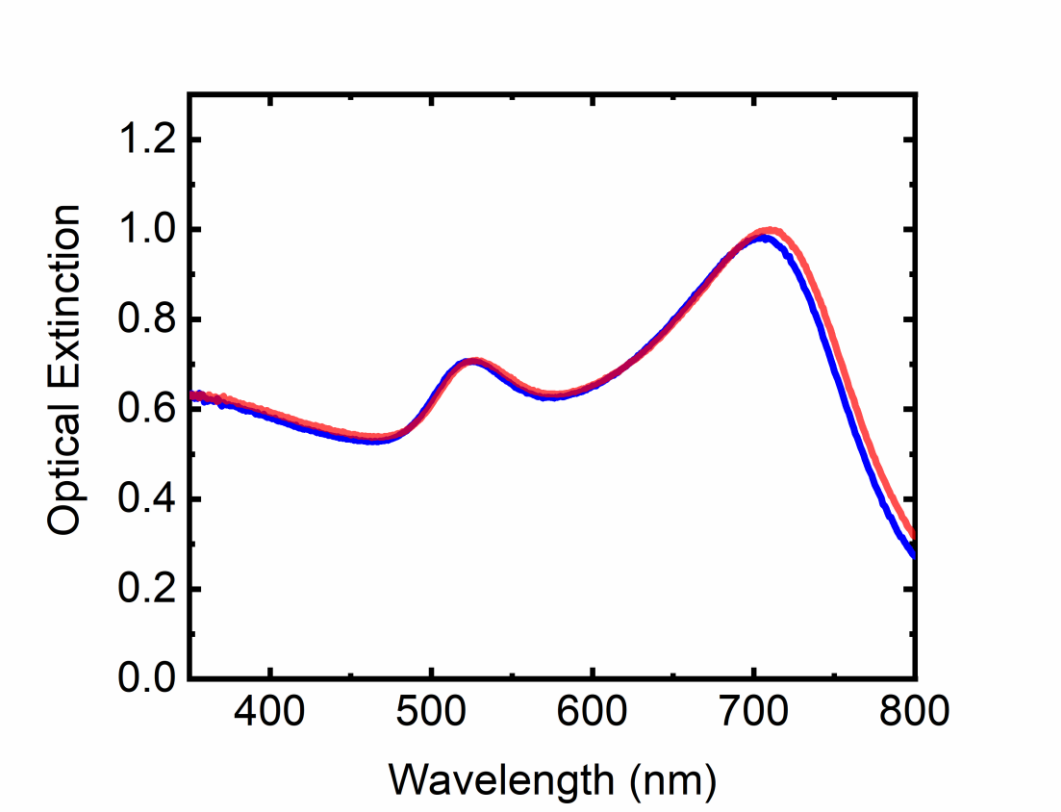

Figure S1. Self-assembled Au nanobead chains with 705 nm peak (blue) and 710 nm peak (red) longitudinal SPR.

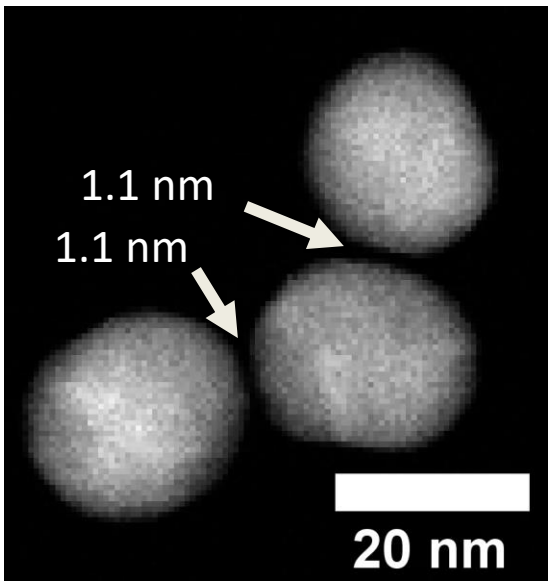
1.1 nm
1.1 nm
20 nm

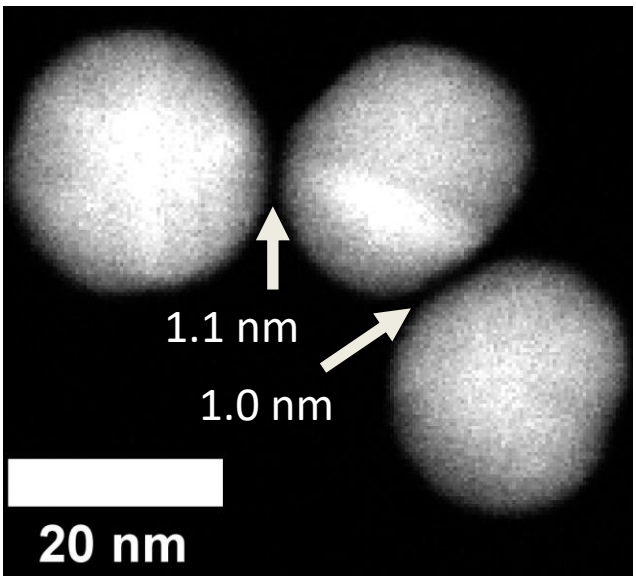
1.1 nm
1.0 nm
20 nm

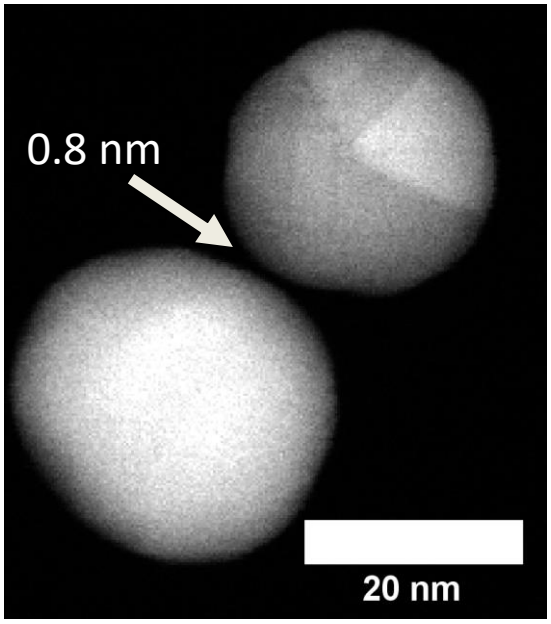
0.8 nm
20 nm

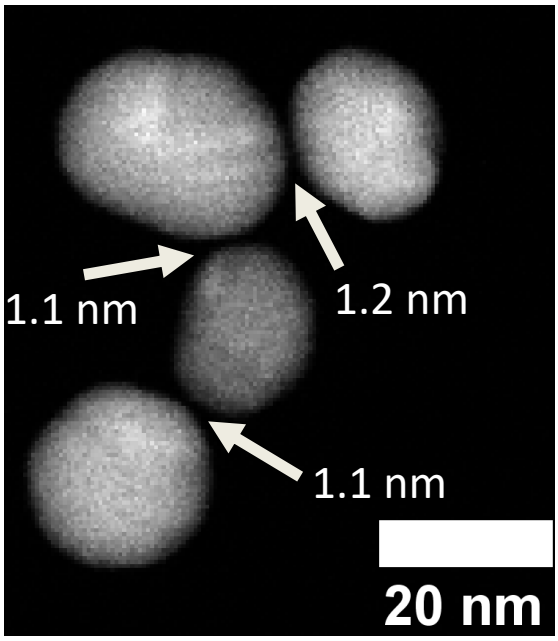
1.1 nm
1.2 nm
1.1 nm
20 nm

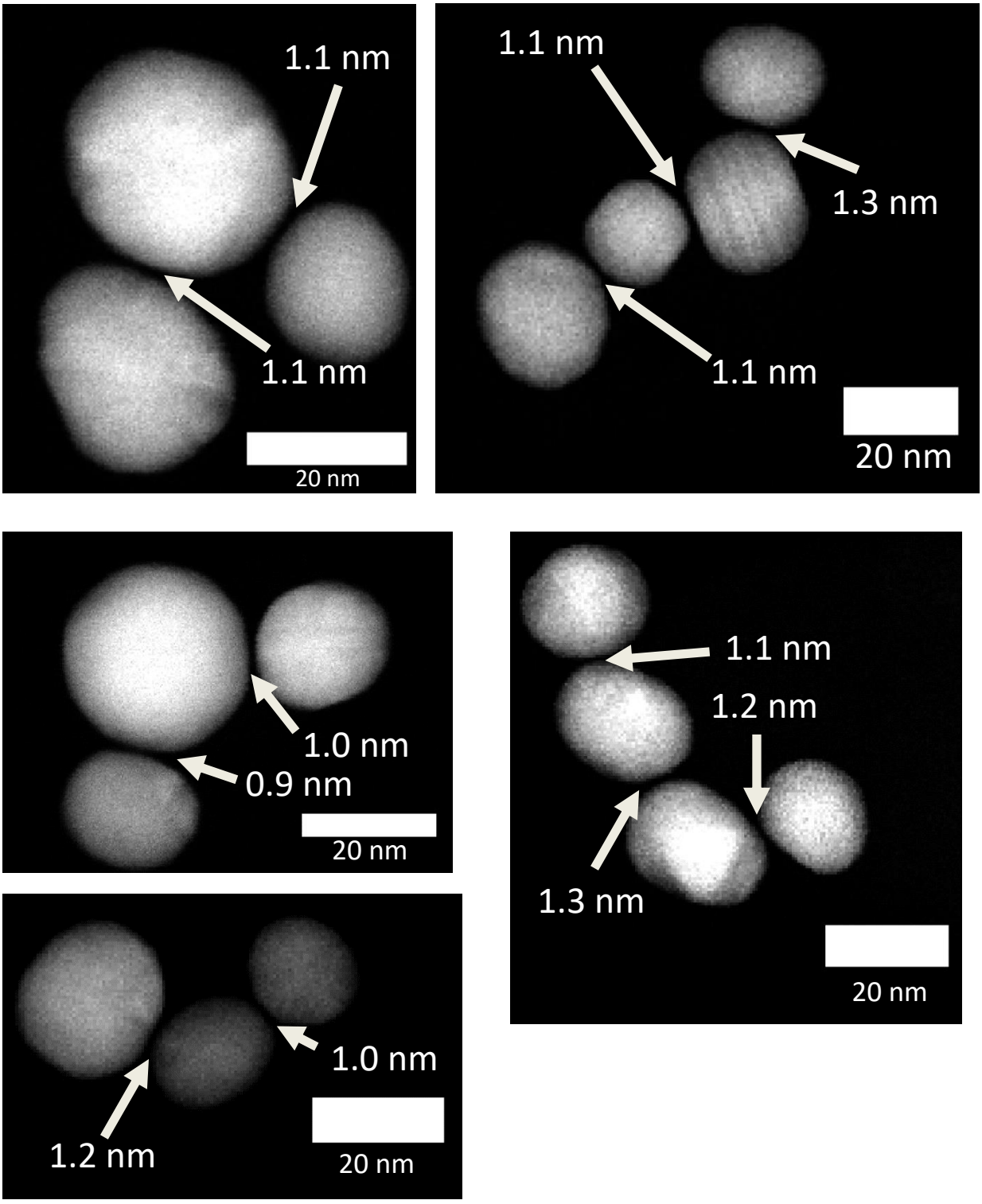

Figure S2. High-resolution TEM images of Au nanobead chains, revealing narrow gap distances (0.80 – 1.3 nm), with an average gap distance of 1.1 nm ± 0.1 nm.

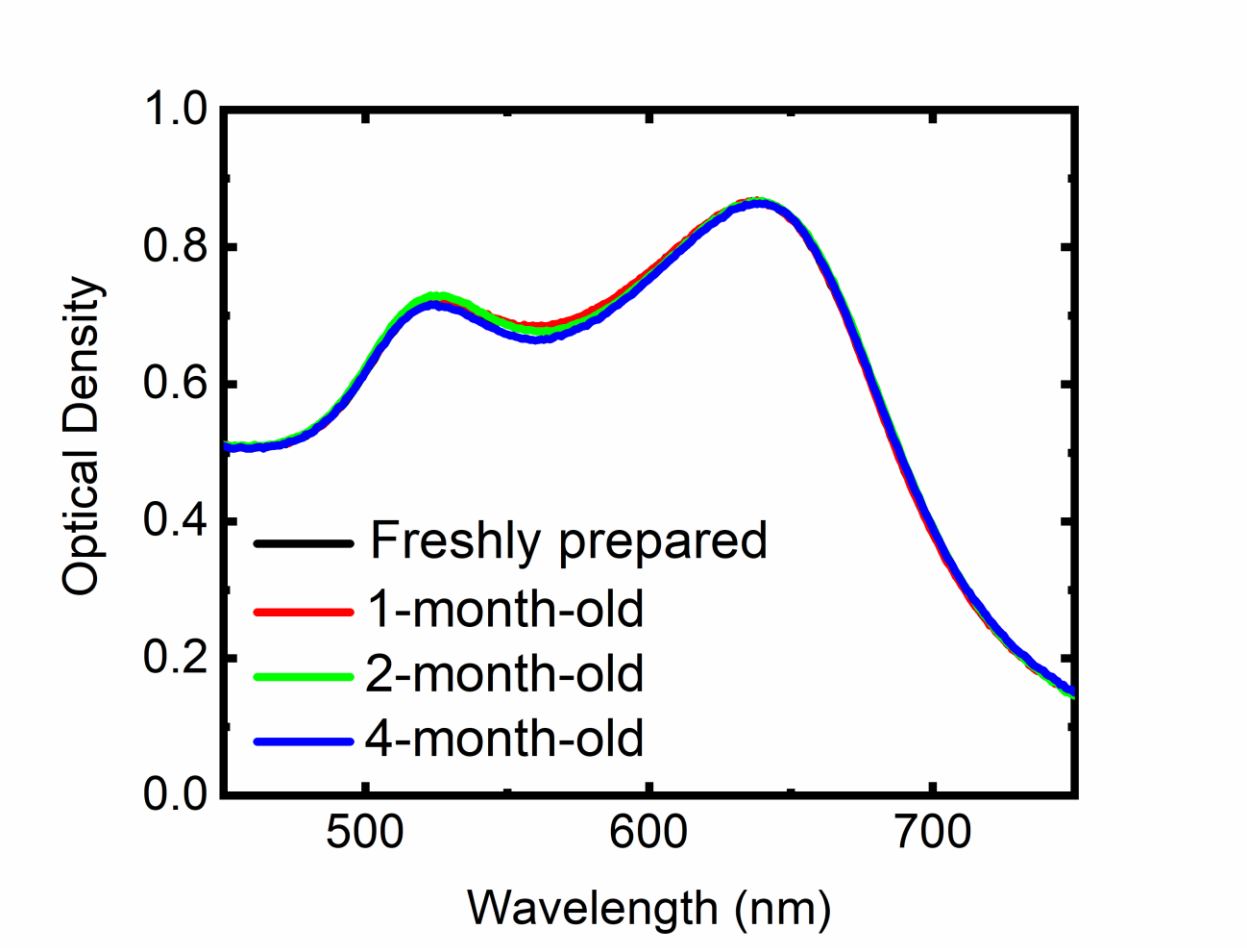

Figure S3. UV-Vis spectra of 640 nm Au nanobead chain immediately after preparation, and 1, 2, and 4 months after preparation. The black line cannot be seen, as it lies behind the red line. The UV-Vis spectra do not significantly change, indicating that the nanochain sample integrity is maintained.

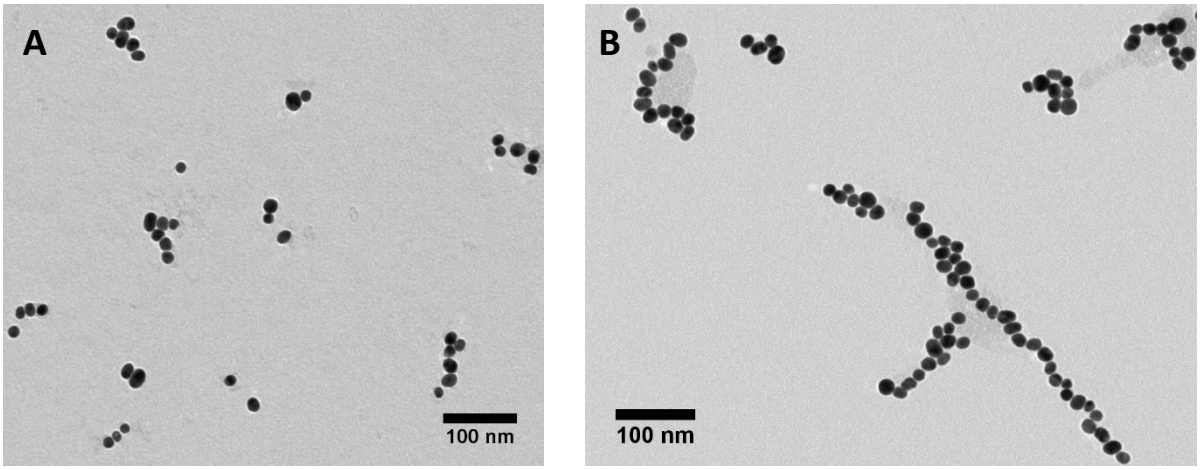

Figure S4. TEM images of A.) 610 nm longitudinal SPR and B.) 640 nm longitudinal SPR samples prepared in a 2nd batch. As the images demonstrate, using UV-Vis to select for the longitudinal surface plasmon wavelength produces particles of comparable morphologies and lengths across batches (i.e. allows for intra-particle reproducibility).

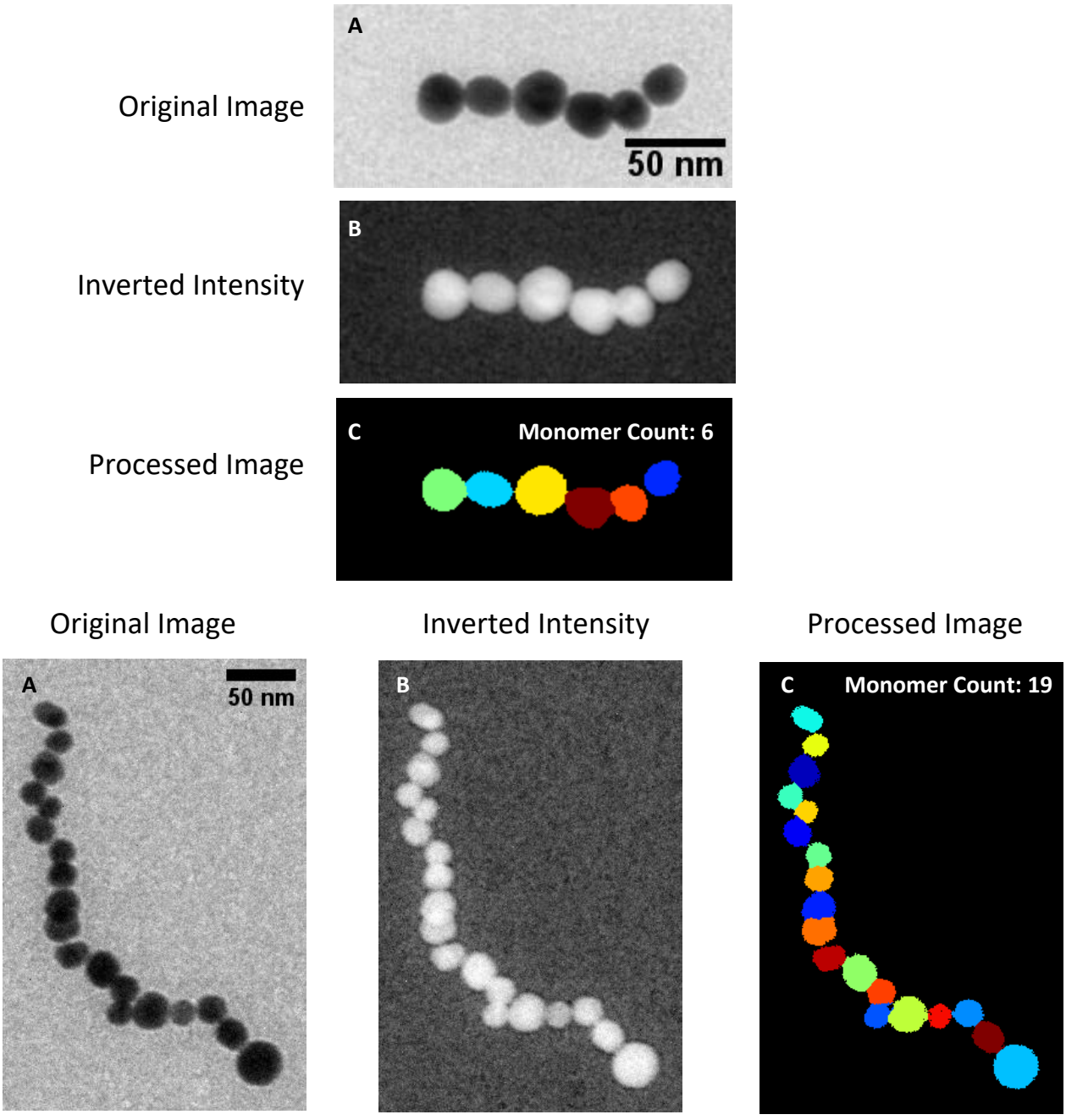

Figure S5. Nanobead chains processed through CellProfiler. For each nanochain pair, the A.) original image (no scale bar) is B.) inverted, and then C.) processed through CellProfiler, where each unique color is an identified counted monomer (60% thresholds shown in processed image).

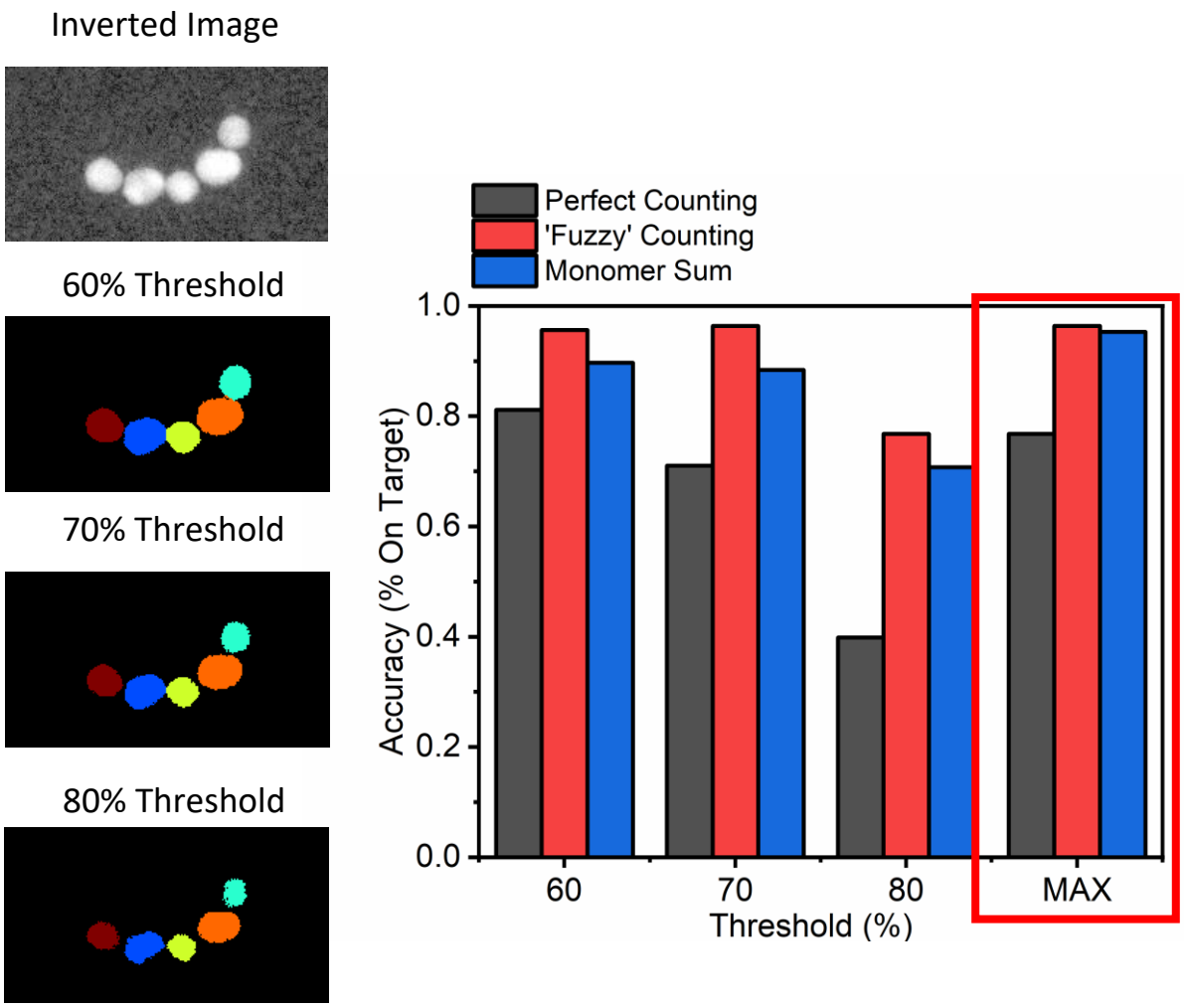

Figure S6. (Left) CellProfiler processing across different intensity thresholds (60, 70, and 80%). To determine the monomer units in the chain, the maximum count number ('MAX') between 60, 70, and 80% intensity thresholds were taken to determine chain length. (Right) CellProfiler accuracies of 60, 70, 80, and 'MAX' thresholding. Perfect counting is defined as counting that differs by 0 between CellProfiler and the operator (human). 'Fuzzy' counting is defined as counting that differs by ±1 between CellProfiler and the operator. Monomer sum is defined as the % of total monomers (across all chains) counted by CellProfiler as a ratio to the operator. As the monomer sum data shows, CellProfiler has a consistent tendency to underestimate chain length in relation to the operator across all thresholds (60-80%). This

outcome supports using the 'MAX' thresholding to classify samples, which achieve 76% accuracy for perfect counting, and >96% accuracy for fuzzy counting.

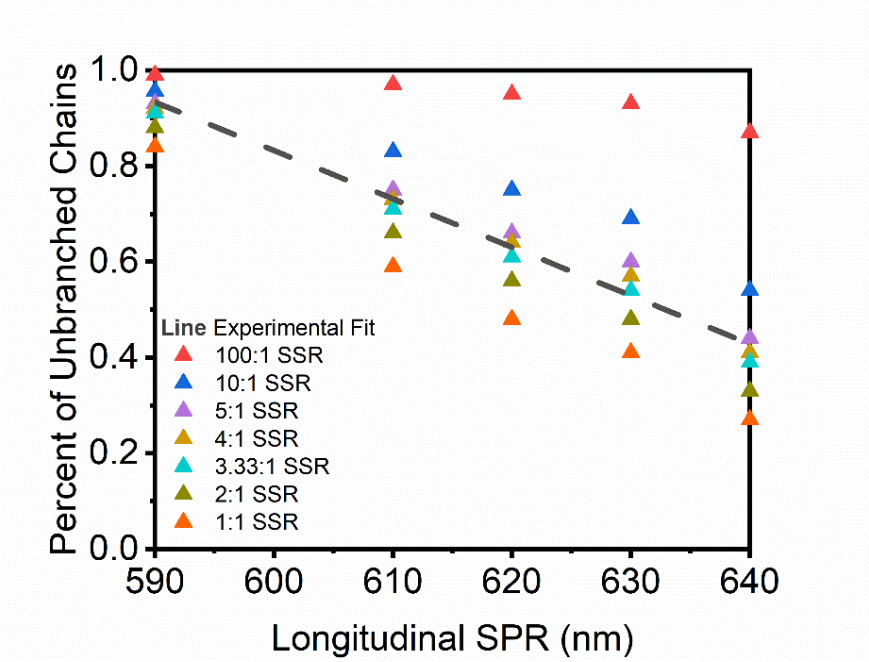

Figure S7A. Percent of unbranched chains for various simulated sticking ratios ('SSR') under 1/m inverse mass dependence diffusion from 590 nm to 640 nm longitudinal SPR. The grey dashed line is the experimental best-fit from the nanochain samples.

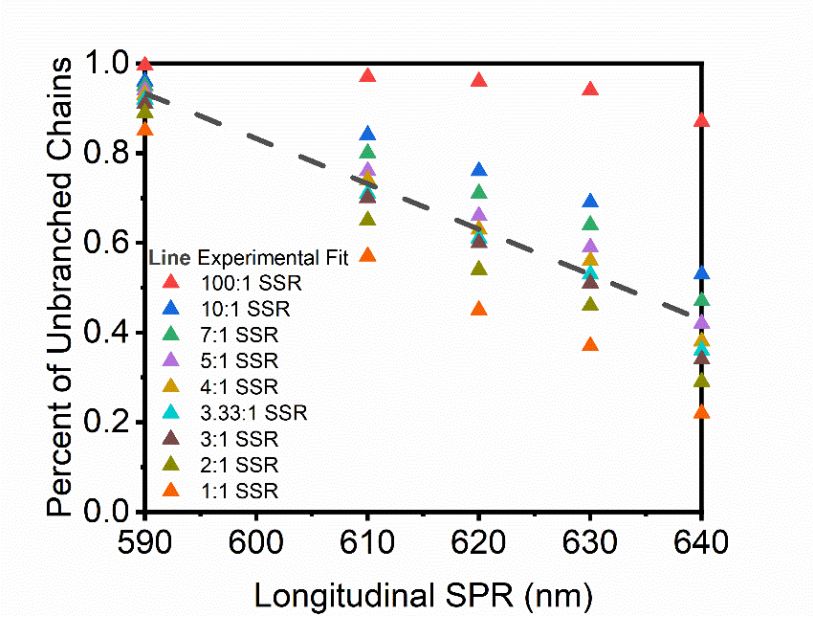

Figure S7B. Percent of unbranched chains for various simulated sticking ratios ('SSR') under $1/m^{1.5}$ inverse mass dependence diffusion from 590 nm to 640 nm longitudinal SPR. The grey dashed line is the experimental best-fit from the nanochain samples.

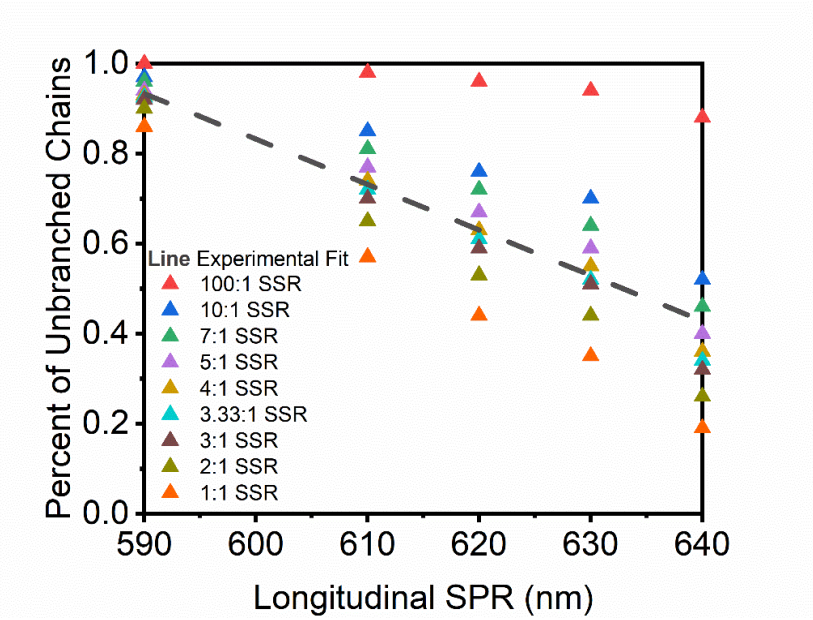

Figure S7C. Percent of unbranched chains for various simulated sticking ratios ('SSR') under $1/m^2$ inverse mass dependence diffusion from 590 nm to 640 nm longitudinal SPR. The grey dashed line is the experimental best-fit from the nanochain samples.

Due to file size, directly uploaded on ACS Portal.

anim640nm4to1m15.avi

Figure S8A. Monte Carlo simulation under $1/m^{1.5}$ inverse mass diffusion for assembly of 640 nm longitudinal SPR nanobead chains under a 4:1 *head-to-center* sticking bias.

Due to file size, directly uploaded on ACS Portal.

anim640nm4to1m2.avi

Figure S8B. Monte Carlo simulation under $1/m^2$ inverse mass diffusion for assembly of 640 nm longitudinal SPR nanobead chains under a 4:1 *head-to-center* sticking bias.

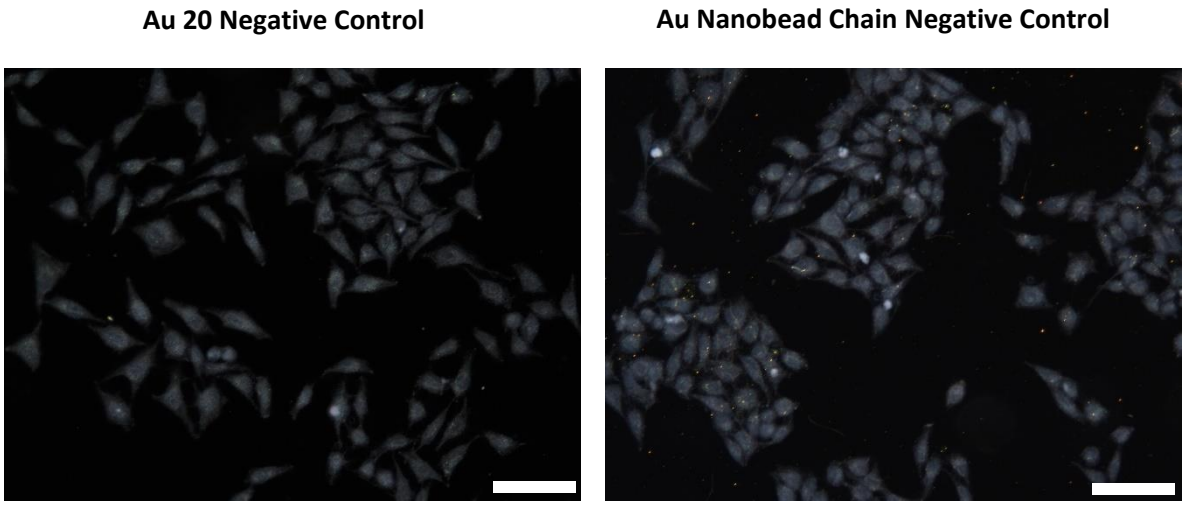

Figure S9. Dark-field light scattering images of human HeLa cancer cells stained with (left) 20 nm NP monomers (no RGD peptide surface conjugated) and (right) Au nanochains with longitudinal SRP at 640 nm (no RGD peptide surface conjugated). The scale bar is 100 µm.

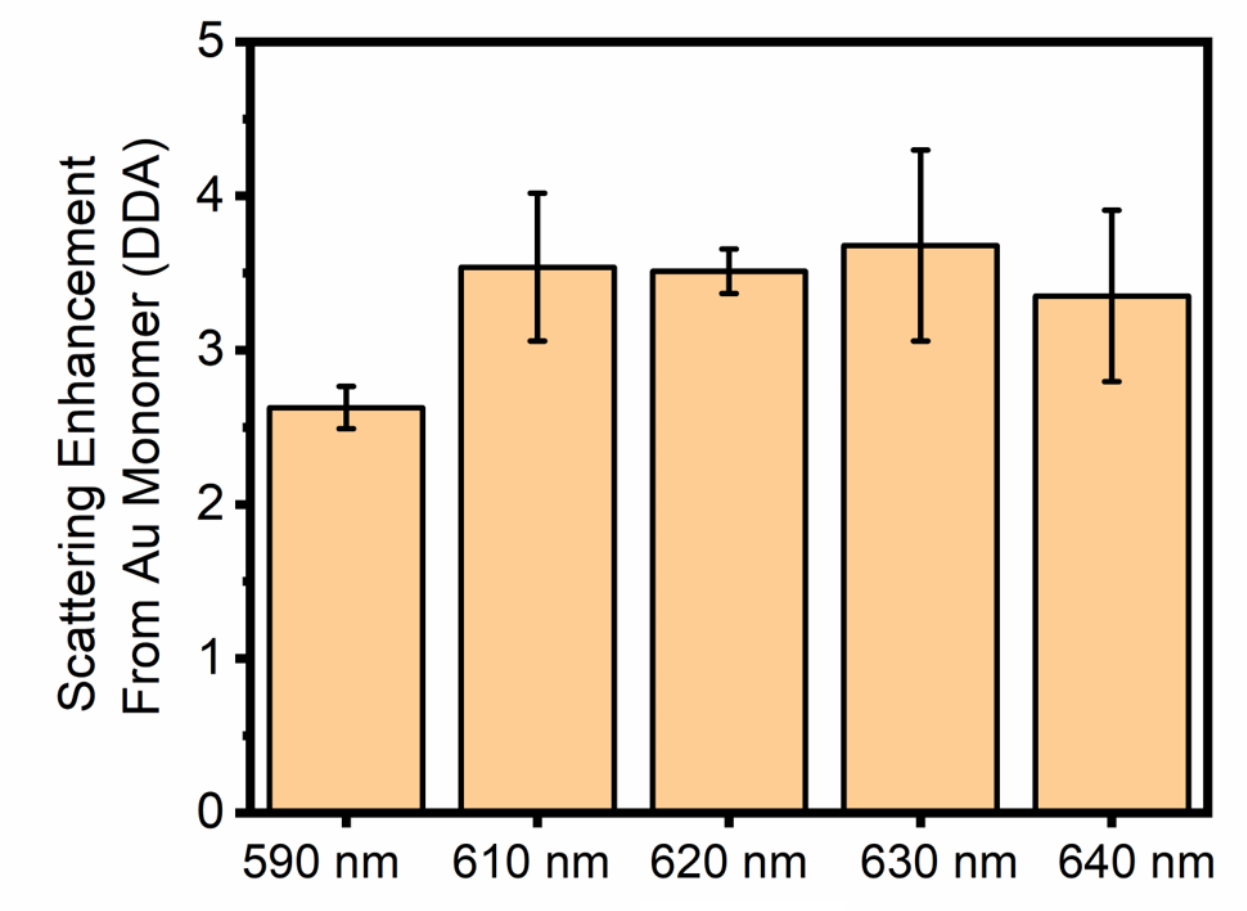

Figure S10. Computed (DDA) scattering enhancement for 590 nm, 610 nm, 620 nm, 630 nm, and 640 nm longitudinal SPR nanobead chains under excitation from a tungsten halogen (500 – 700 nm excitation) lamp per nanosphere as compared to a 20 nm Au monomer (525 nm longitudinal SPR).

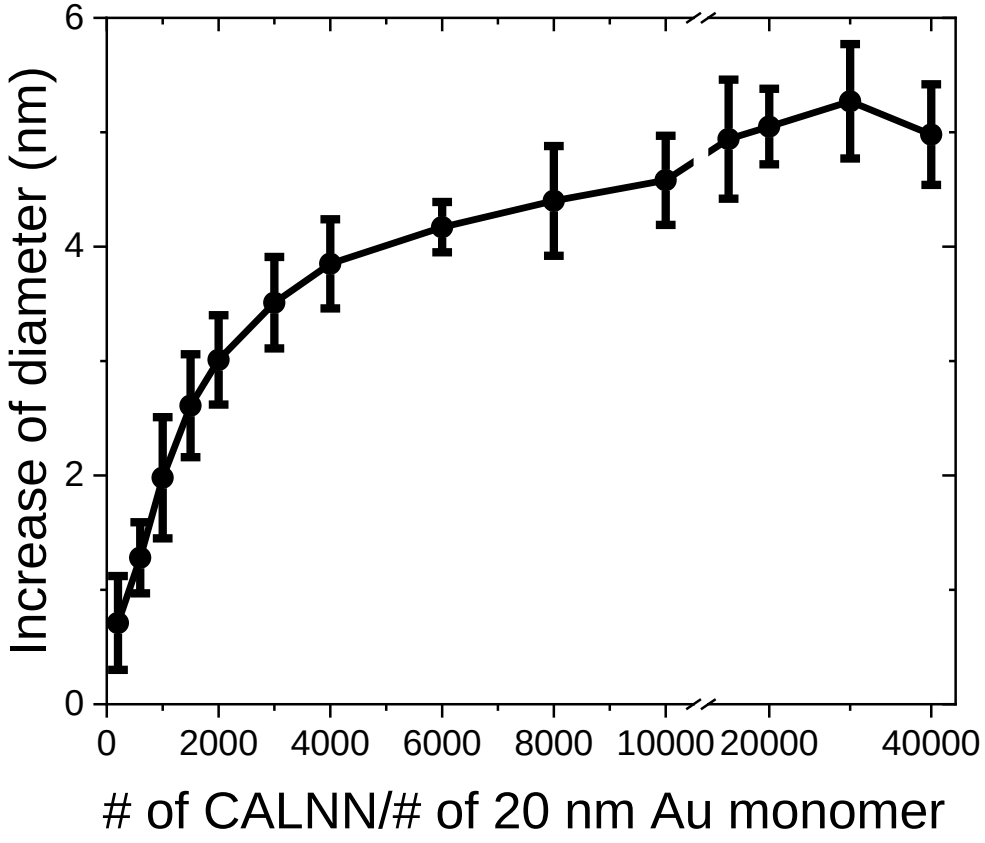

Figure S11. Increased diameter (nm) of 20 nm Au monomers after CALNN peptide conjugation at various CALNN molar conjugation ratios (200:1-40000:1) determined through dynamic light scattering (DLS). Beyond a 20000:1 CALNN:Au ratio, the Au monomer no longer exhibits increases in diameter, indicating that the Au monomer has complete peptide surface coverage.

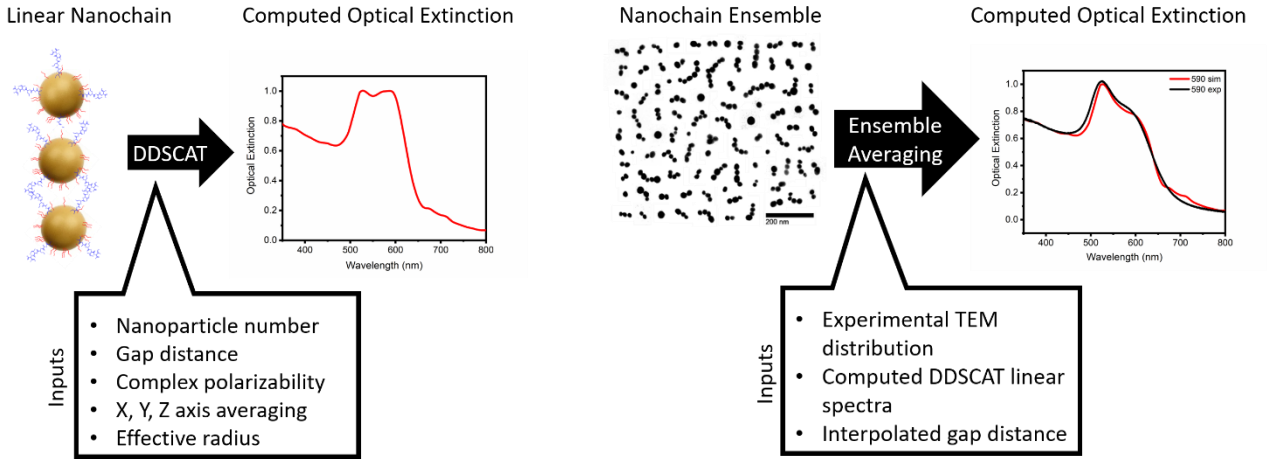

Figure S12. Protocol used to compute the optical extinction spectra of the nanochain ensemble. First, the optical extinction spectrum of each linear nanochain is computed via DDSCAT assuming unpolarized excitation (left diagram with example spectrum). Next, ensemble averaging is performed utilizing TEM distributions to generate a simulated spectra (red) compared to an experimental spectra (black).

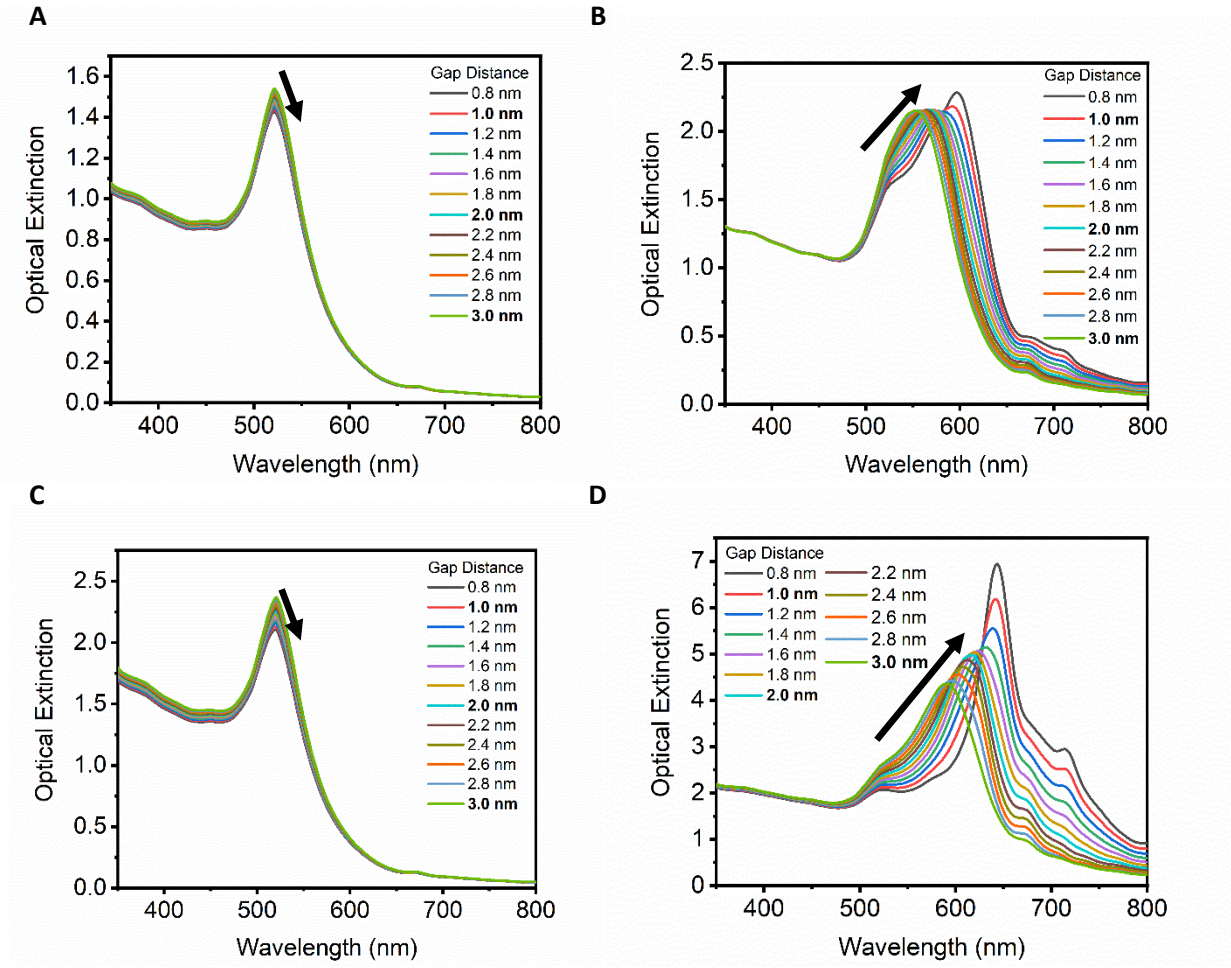

Figure S13. Optical extinction spectra for a trimer chain (A-B) and 15-mer chain (C-D) samples along the x orientation (no longitudinal SPR; Figures 10A, C) the yz orientations (where longitudinal SPR will be observed; Figures 10B, D) with interpolated gap distances every 0.2 nm utilizing 1.0, 2.0, and 3.0 nm indices (indices are bolded in the figure legends). It is observed that the spectra from the interpolated gap distances are continuous and exhibit the expected plasmonic red-shifting in both magnitude and direction as gap distance gets smaller (labeled with the black arrows), indicating that the polynomial interpolation method can be used for this dataset.